Electrically Tunable Distributed Feedback Laser Emission from Scaffolding Morphologic Holographic Polymer Dispersed Liquid Crystal Grating

2013 Appl. Phys. Express 6 022702

(http://iopscience.iop.org/1882-0786/6/2/022702)

Applied Physics Express 6 (2013) 022702
http://dx.doi.org/10.7567/APEX.6.022702

Electrically Tunable Distributed Feedback Laser Emission from Scaffolding Morphologic Holographic Polymer Dispersed Liquid Crystal Grating

Wenbin Huang[1,2], Zhihui Diao[1,2], Lishuang Yao[1], Zhaoliang Cao[1], Yonggang Liu[1], Ji Ma[1,3*], and Li Xuan[1*]

[1]*State Key Laboratory of Applied Optics, Changchun Institute of Optics, Fine Mechanics and Physics, Chinese Academy of Sciences, Changchun 130033, China*
[2]*Graduate School of Chinese Academy of Sciences, Beijing 100039, China*
[3]*Liquid Crystal Institute, Kent State University, Kent, OH 44240, U.S.A.*
E-mail: jma2@kent.edu; xuanli@ciomp.ac.cn

Received December 9, 2012; accepted January 4, 2013; published online January 25, 2013

Electrically tunable distributed feedback (DFB) laser emission from a dye-doped holographic polymer dispersed liquid crystal (HPDLC) transmission grating is demonstrated. The homogenously aligned liquid crystal (LC) in this polymer scaffolding morphologic grating enables a large refractive index (RI) change for the TM wave under applied electric field, which in turn leads to a red-shift of 8 nm in the output laser emission. The tuning behavior of the DFB laser is well explained on the basis of DFB waveguide theory and amount of phase-separated LCs.

Recently, organic solid-state lasers (OSSLs) have attracted broad scientific interest.[1)] One of the main reasons is that organic materials offer a broad gain spectrum, which the inorganic ones cannot provide. The broad gain spectrum shows the opportunity of making low-cost, tunable lasers for applications like optical communication and spectroscopy.[2,3)] Among OSSLs, the distributed feedback (DFB) structure is one of the most important resonator configurations, because it exhibits low threshold and stable laser operation. The DFB laser wavelength λ_{laser} with a grating period Λ fulfills the Bragg equation $\lambda_{laser} = 2\Lambda n_{eff\_mode}/m_{Bragg}$, where m_{Bragg} is the Bragg order and n_{eff_mode} is the effective refractive index (RI) of the lasing mode.[4)] Thus, the DFB lasers can achieve tunable properties by changing the grating period or effective RI, such as using a wedge-shape film of the gain medium layer or the intermediate high-index layer,[5,6)] mechanically stretchable gratings,[7,8)] electroactive elastomer actuator grating,[9)] photochromic additive incorporated in the gain medium,[10)] and using liquid crystal (LC) in the waveguide core layer[11–13)] or cladding layer.[14)]

LCs are electro-optical birefrigent materials that their orientation can be changed by an electric field, and thus they have the potential for making electrically tunable DFB lasers. Compared with other tuning approaches, using LCs allows the lasing wavelength to be tunable without moving the sample or altering the pumping setup. The holographic polymer dispersed liquid crystal (HPDLC) grating, made by photopolymerization-induced phase separation, is a thin film composed of alternating layers of LC- and polymer-rich lamellas.[15,16)] They have merits such as ease of fabrication, low-cost, and large processing area. Distributed feedback laser action has been demonstrated in dye-doped HPDLC reflection grating or transmission grating,[17,18)] and electrical switching of laser action in HDPLCs has also been demonstrated,[19,20)] but studies on the electrical tuning of the lasing wavelength in HPDLC gratings are insufficient.[21)]

In this work, we present an electrically tunable organic laser with a lasing tuning range of 8 nm by using a polymer scaffolding morphologic HPDLC transmission grating as the resonator. The phase-separated LCs are homogenously aligned along the grating vector,[22)] and their alignment can be changed by an electric field, resulting in the lasing wavelength tunable behavior. The tuning range presented here is comparable to the electrical tuning of 10 nm by filling LCs into a nano-imprinted structure[12)] and higher than 4.7 nm by using a mechanically stretchable polymer[8)] or 4 nm by incorporating LCs in the cladding layer.[5)] Furthermore, a theoretical model is established on the basis of the DFB waveguide theory to explain our result, and it is found that our experimental results are in good agreement with theoretical calculations.

The polymer scaffolding morphologic HPDLC transmission grating was made from a prepolymer mixture composed of phthalic diglycol diacrylate monomer (PDDA; 28.5 wt %, Xiyachem), dipentaerythritol hydroxyl pentaacrylate monomer (DPHPA; 29 wt %, Sigma-Aldrich), *N*-vinylpyrrolidone (NVP; 10 wt %, Sigma-Aldrich), nematic LC TEB30A (30 wt %, Silichem), coinitiator *N*-phenyglycine (NPG; 1.5 wt %, Sigma-Aldrich), photoinitiator Rose Bengal (RB; 0.5 wt %, Sigma-Aldrich), and laser dye 4-dicyanmethylene-2-methyl-6-(*p*-dimethylaminostyryl)-4*H*-pyran (DCM; 0.5 wt %, Sigma-Aldrich). The homogeneous mixture was injected into an empty cell and was exposed to the interference patterns created by two coherent 532 nm laser beams (8 mW/cm^2 per beam, 5 min). The detailed experimental setup can be found in our previous reports.[22–24)] The polymerization-induced phase separation results in a microstructure with alternating layers of polymer and LC, as shown in Fig. 1(a), where the phase separated LC is initially aligned along the grating vector due to the anchoring effect of polymer filaments.[22)] The low exposure intensity is crucial to achieving this polymer scaffolding morphologic grating, and thanks to the absence of LC domains, this grating shows merely scattering and is particularly suitable as a laser cavity.

The LC cell thickness is controlled to be as low as 3 μm because the thicker cell will increase the number of allowed modes, and make it difficult to distinguish the electrically tuned lasings. A thin film (30 nm) of indium tin oxide (ITO) is coated over the glass to apply an electric field. Experimentally, we found that the ITO layer is too thin to form an effective optical layer, and the DFB waveguide structure can be regarded as the high-RI core layer (HPDLC grating) cladded by the two low-RI cladding glass substrates [Fig. 1(d)]. The RIs of materials used in this work are measured and given as follows: ordinary RI of the LC (n_o) is

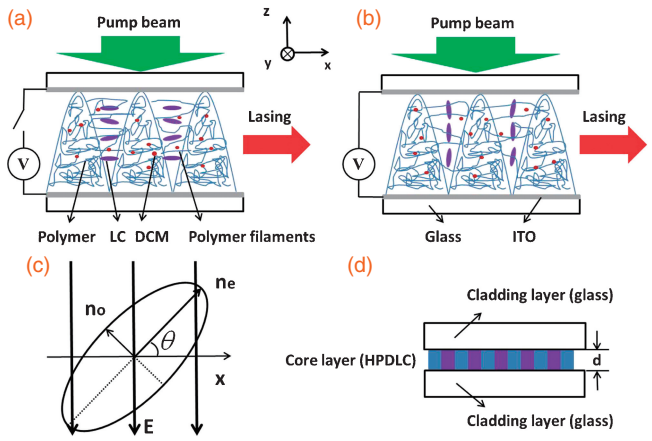

Fig. 1. Schematic representation of the HPDLC grating for electrically tunable lasing: (a) without field, (b) with field, (c) orientation of the LC, and (d) equivalent waveguide structure.

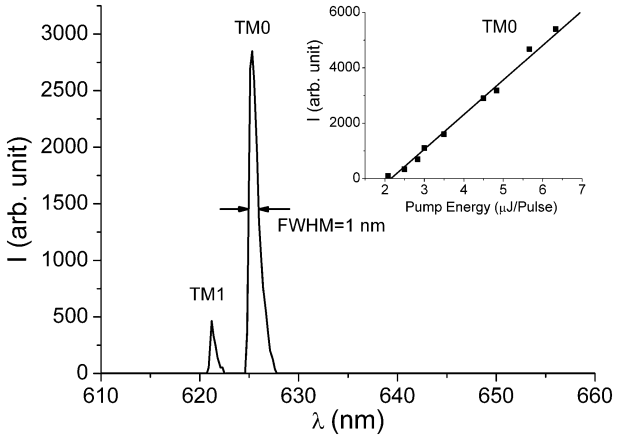

Fig. 2. Emission spectrum at 4.5 μJ/pulse without the application of voltage. Inset: dependence of TM_0 peak intensity on pump energy.

1.522, extraordinary RI of the LC (n_e) is 1.692, RI of the pure polymer n_p is 1.534, and RI of the cladding layer (glass) $n_{cladding\_layer}$ is 1.516.

The HPDLC grating period was chosen as 609.0 nm. According to the Bragg equation and DCM gain property, this period will allow the third DFB laser emission occurrence at ~625 nm, which falls in the center of the DCM gain spectrum.[24] A power supply was used to apply an electric field (rectangular signal: 1 kHz frequency) to continuously control the orientation of the LCs when the sample was being optically pumped by a 532 nm Q-switched neodymium-doped yttrium aluminum garnet (Nd:YAG) pulsed laser (pulse duration: 8 ns; repetition rate: 8 Hz). The electrically tunable lasing output was detected by a fiber-coupled spectrometer, and a polarizer was placed before the fiber to allow only TM laser emission to be collected.

The achieved laser emission and dependence of TM_0 peak intensity on the pump energy are shown in Fig. 2. The full-width at half maximum (FWHM) of each peak is around 1 nm, confirming the lasing behaviors from our grating. Figure 3 shows the laser emission spectra from our dye-doped HPDLC at different applied electric fields. The lasing wavelength began to redshift from 625.1 nm when the field

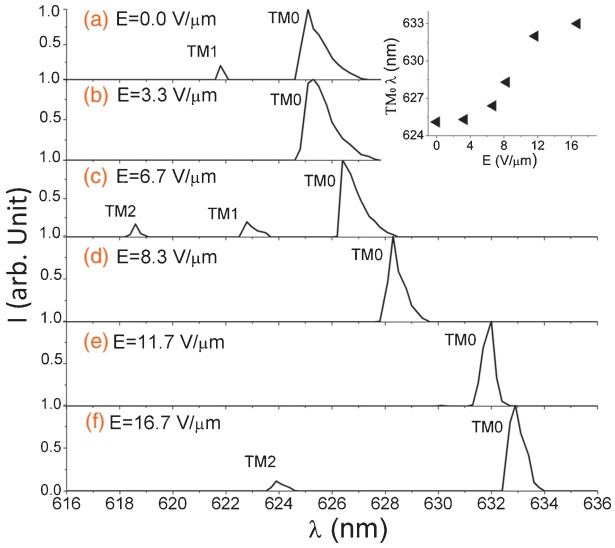

Fig. 3. Lasing spectra from dye-doped HDPLC at different electric fields. Inset: TM_0 lasing wavelength as a function of applied electric field.

exceeded 3.3 V/μm, where the LCs overcame the anchoring of the polymer filaments to rotate in the x–z plane. When the electric field was saturated (16.7 V/μm), the peak of the TM_0 mode lasing was tuned to 633.1 nm, showing a total 8 nm redshift. The required electric field here is much lower than that in a 2D HPDLC grating (42 V/μm for 5 nm blue shift).[21] We can also find the higher order modes redshifted upon application of the electric field. For example, the TM2 mode lasing showed a 5 nm tunable range from 619.0 nm [Fig. 3(c)] to 624.0 nm [Fig. 3(f)].

Upon application of an electric field, the LC begins to reorient to the z-direction in the x–z plane [Figs. 1(b) and 1(c)]. During this procedure, the effective RI of the LC n_{eff_LC} is equal to $n_o n_e / \sqrt{n_e^2 \cos^2\theta + n_o^2 \sin^2\theta}$, where θ is the angle between the LC molecule and the x-direction that can be changed from 0 to 90° by the field. The change in the effective RI in the LC will lead to a shift in the DFB lasing wavelength in the equivalent waveguide structure [Fig. 1(d)].

To further explain the experimental results, a quantitative understanding of the change in the effective RI of the waveguide core layer induced by the electric field is given here. For the TM wave propagating along the x-direction in the grating, the effective RI of the core layer n_{core_layer} can be expressed as

$$n_{core\_layer} = [n_p^2 \times \varphi_p + n_{eff\_LC}^2 \times \varphi_{LC} + (2n_o^2/3 + n_e^2/3) \times (1 - \varphi_p - \varphi_{LC})]^{1/2}, \quad (1)$$

where φ_p, φ_{LC}, and $1 - \varphi_p - \varphi_{LC}$ are the volume proportions of the pure polymer, the phase-separated LCs, and the LCs dissolved in the polymer, respectively. φ_p is 0.7 determined using the monomer concentration in the mixture, and φ_{LC} is 0.11 determined by the birefringence measurement method.[22] For the DFB waveguide laser, the output lasing mode has to meet two conditions. One condition is that the light mode should be the allowed mode in the waveguide. That means that the light would not leak out through the adjacent cladding layer (glass substrate). We fulfill the waveguide equation[25] using the parameters from our DFB structure as

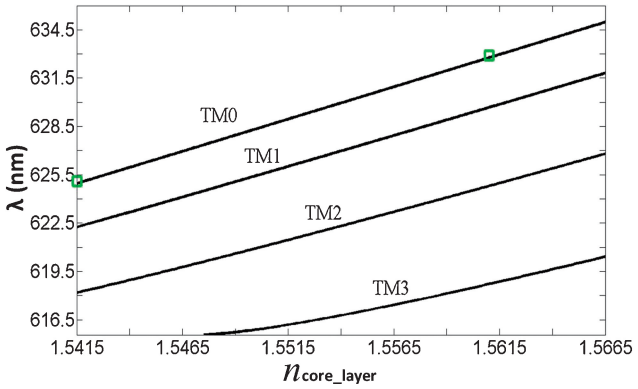

Fig. 4. Lasing wavelength as a function of effective RI of the core layer. Green squares: experimental data.

$$\frac{\pi d}{\lambda}\sqrt{n_{\text{core\_layer}}^2 - n_{\text{eff\_mode}}^2} = \frac{m_{\text{mode}}\pi}{2} + \arctan\left(\frac{n_{\text{core\_layer}}^2}{n_{\text{cladding\_layer}}^2}\sqrt{\frac{n_{\text{eff\_mode}}^2 - n_{\text{cladding\_layer}}^2}{n_{\text{core\_layer}}^2 - n_{\text{eff\_mode}}^2}}\right), \quad (2)$$

where d is the core layer thickness (3 μm), m_{mode} $(= 0, 1, 2, \ldots)$ is the order of the waveguide mode, and λ is the wavelength of the mode in free space. The other condition is that the mode needs to satisfy the Bragg equation $2n_{\text{eff\_mode}}\Lambda = 3\lambda$ (judging from the experimental result, our laser emission is from the third Bragg order). Therefore, the light can form a standing wave in the cavity via the coherent reflections in this periodic structure, be further amplified by the stimulated emission as they are travelling around, and become lasing when the pumping energy exceeds the threshold.

Through Eq. (2) and the satisfied Bragg equation, the allowed lasing wavelength can be numerically solved, and its value as a function of $n_{\text{core\_layer}}$ is calculated and shown in Fig. 4. The parameters used in the calculation are mentioned in the experimental part. In order to compare the experimental results with theoretical calculation, we consider two extremes for TM_0 lasing mode: (a) without applied electric field, $n_{\text{eff\_LC}} = n_o = 1.522$ and $n_{\text{core\_layer}} = 1.5416$ using Eq. (1). The experimental TM_0 lasing located at 625.1 nm [Fig. 3(a)] is in good agreement with the theoretical curve; and (b) with a saturated electric field, the LCs are aligned along the z-direction, $n_{\text{eff\_LC}} = n_e = 1.692$ and $n_{\text{core\_layer}} = 1.5610$. Experimentally, the TM_0 lasing was electrically tuned to 633.1 nm [Fig. 3(f)], which also agrees with the theoretical calculation. From the experimental and theoretical results, we verify the electrically tunable capability of the lasing from one-dimensional dye-doped HPDLC. Moreover, if the phase-separated LC degree or the birefringence of the LC can be increased, the electrical tuning range can be further enlarged.

In conclusion, we demonstrate electrically tunable DFB laser emission using a dye-doped HPDLC transmission grating and a redshift of 8 nm is achieved. The anchoring effect of the polymer filaments is beneficial for aligning the phase-separated LCs in the grating vector direction initially, which induces a large LC RI change upon application of an electric field, resulting in an electrically tunable property. The phase-separated LCs and waveguide DFB laser theory are used to explain the experimental results, and the experimental results are in good agreement with theoretical calculations.

Acknowledgment This work was supported by the National Natural Science Foundation of China (Grant Nos. 60736042, 11174274, and 11174279).

1) I. D. W. Samuel and G. A. Turnbull: Chem. Rev. **107** (2007) 1272.
2) J. Clark and G. Lanzani: Nat. Photonics **4** (2010) 438.
3) Y. Oki, S. Miyamoto, M. Maeda, and N. J. Vasa: Opt. Lett. **27** (2002) 1220.
4) T. Matsui, M. Ozaki, and K. Yoshino: J. Opt. Soc. Am. B **21** (2004) 1651.
5) S. Klinkhammer, X. Liu, K. Huska, Y. S. Vanderheiden, S. Valouch, C. Vannahme, S. Bräse, T. Mappes, and U. Lemmer: Opt. Express **20** (2012) 6357.
6) M. Stroisch, T. Woggon, C. Teiwes-Morin, S. Klinkhammer, K. Forberich, A. Gombert, M. Gerken, and U. Lemmer: Opt. Express **18** (2010) 5890.
7) B. Wenger, N. Tétreault, M. E. Welland, and R. H. Friend: Appl. Phys. Lett. **97** (2010) 193303.
8) P. Görrn, M. Lehnhardt, W. Kowalsky, T. Riedl, and S. Wagner: Adv. Mater. **23** (2011) 869.
9) S. Döring, M. Kollosche, T. Rabe, J. Stumpe, and G. Kofod: Adv. Mater. **23** (2011) 4265.
10) B. H. Wallikewitz, G. O. Nikiforov, H. Sirringhaus, and R. H. Friend: Appl. Phys. Lett. **100** (2012) 173301.
11) T. Matsui, M. Ozaki, and K. Yoshino: Appl. Phys. Lett. **83** (2003) 422.
12) R. Ozaki, T. Shinpo, K. Yoshino, M. Ozaki, and H. Moritake: Appl. Phys. Express **1** (2008) 012003.
13) R. Ozaki, T. Shinpo, H. Moritake, K. Yoshino, and M. Ozaki: Mol. Cryst. Liq. Cryst. **507** (2009) 234.
14) S. Klinkhammer, N. Heussner, K. Huska, T. Bocksrocker, F. Geislhöringer, C. Vannahme, T. Mappes, and U. Lemmer: Appl. Phys. Lett. **99** (2011) 023307.
15) R. L. Sutherland, L. V. Natarajan, V. P. Tondiglia, T. J. Bunning, and W. W. Adams: Appl. Phys. Lett. **64** (1994) 1074.
16) R. Caputo, L. D. Sio, A. Veltri, C. Umeton, and A. V. Sukhov: Opt. Lett. **29** (2004) 1261.
17) R. Jakubiak, T. J. Bunning, R. A. Vaia, L. V. Natarajan, and V. P. Tondiglia: Adv. Mater. **15** (2003) 241.
18) Y. J. Liu, X. W. Sun, P. Shum, H. P. Li, J. Mi, and W. Ji: Appl. Phys. Lett. **88** (2006) 061107.
19) R. Jakubiak, L. V. Natarajan, V. P. Tondiglia, G. S. He, P. N. Prasad, T. J. Bunning, and R. A. Vaia: Appl. Phys. Lett. **85** (2004) 6095.
20) V. K. S. Hsiao, C. Lu, G. S. He, M. Pan, A. N. Cartwright, P. N. Prasad, R. Jakubiak, R. A. Vaia, and T. J. Bunning: Opt. Express **13** (2005) 3787.
21) R. Jakubiak, V. P. Tondiglia, L. V. Natarajan, R. L. Sutherland, P. Lloyd, T. J. Bunning, and R. A. Vaia: Adv. Mater. **17** (2005) 2807.
22) W. Huang, Y. Liu, Z. Diao, C. Yang, L. Yao, J. Ma, and L. Xuan: Appl. Opt. **51** (2012) 4013.
23) W. Huang, Z. Diao, Y. Liu, Z. Peng, C. Yang, J. Ma, and L. Xuan: Org. Electron. **13** (2012) 2307.
24) Z. Diao, S. Deng, W. Huang, L. Xuan, L. Hu, Y. Liu, and J. Ma: J. Mater. Chem. **22** (2012) 23331.
25) K. Okamoto: *Fundamentals of Optical Waveguides* (Academic Press, San Diego, CA, 2006) 2nd ed., p. 26.